

Two-dimensional mapping of the asymmetric lateral coherence of thermal light

B. PAROLI* AND M.A.C. POTENZA

Dipartimento di Fisica, Università degli Studi di Milano and INFN Sezione di Milano - via G. Celoria, 16, 20133 Milano, Italy

*bruno.paroli@unimi.it

Abstract: We report in this work the first experimental verification of the asymmetric lateral coherence which is a measurement of the spatio-temporal coherence by using a wide-band Young interference experiment with a fixed off-axis slit. We demonstrate the coherence properties through the measurement of the real part of the coherence factor of thermal light. We extend our recent results obtained for betatron and undulator radiations providing a robust experimental method for the two-dimensional mapping of the two-point correlation function of broadband radiation preserving the phase information. The proposed method can be used as a high-sensitivity alternative to traditional interferometry with quasi-monochromatic radiation.

© 2016 Optical Society of America

OCIS codes: (030.1640) Coherence; (340.6720) Synchrotron radiation; (140.7215) Undulator radiation.

References and links

1. M. Born and E. Wolf, *Principles of Optics* (Pergamon Ltd., 1970).
2. J.D. Monnier, "Optical interferometry in astronomy," *Rep. Prog. Phys.* **66**, 789–857 (2003).
3. J.G. Robertson and W.J. Tango, *Very High Angular Resolution Imaging* (Springer Science, 1994).
4. D. D. Nolte, *Optical Interferometry for Biology and Medicine* (Springer, 2012).
5. A. Hofmann, "Electron and proton beam diagnostics with synchrotron radiation," *IEEE Trans. Nucl. Sci.* **28**, 2132 (1981).
6. T. Naito and T. Mitsuhashi, "Very small beam-size measurement by a reflective synchrotron radiation interferometer," *Phys. Rev. Spec. Top. Acc. Beam.* **9**, 122802 (2006).
7. V. Kohn, I. Snigireva, and A. Snigirev, "Direct measurement of transverse coherence length of hard x rays from interference fringes," *Phys. Rev. Lett.* **85**, 2745 (2000).
8. P. Skopintsev, A. Singer, J. Bach, L. Müller, B. Beyersdorff, S. Schleitzer, O. Gorobtsov, A. Shabalin, R. P. Kurta, D. Dzhigaev, O. M. Yefanov, L. Glaser, A. Sakdinawat, G. Grübel, R. Frömter, H. P. Oepen, J. Viefhaus, and I. A. Vartanyants, "Characterization of spatial coherence of synchrotron radiation with non-redundant arrays of apertures," *J. Synchrotron Rad.* **21**, 722–728 (2014).
9. M. D. Alaimo, M. A. C. Potenza, M. Manfredda, G. Geloni, M. Sztucki, T. Narayanan, and M. Giglio, "Probing the transverse coherence of an undulator x-ray beam using brownian particles," *Phys. Rev. Lett.* **103**, 194805 (2009).
10. T. Mitsuhashi, "Recent progress in SR interferometer," in *Proceedings of the International Beams Instrumentation Conference 2012*, Tsukuba, Japan (2012).
11. M. Lyubomirskiy, I. Snigireva, and A. Snigirev, "Lens coupled tunable Young's double pinhole system for hard X-ray spatial coherence characterization," *Opt. Exp.* **24**, 13679 (2016).
12. J. W. Goodman, *Statistical Optics* (John Wiley & Sons, 2000).
13. G. Geloni, E. Saldin, E. Schneidmiller, M. Yurkov, "Transverse coherence properties of x-ray beams in third-generation synchrotron radiation sources," *Nucl. Instr. Meth. Phys. Res. A* **588**, 463–493 (2008).
14. R. Coisson, "Spatial coherence of synchrotron radiation," *Appl. Opt.* **34**, 904–908 (1995).
15. B. Paroli, E. Chiadroni, M. Ferrario, V. Petrillo, M. A. C. Potenza, A. R. Rossi, L. Serafini, and V. Shpakov, "Asymmetric lateral coherence of betatron radiation emitted in laser-driven light sources," *Europhys. Lett.* **111**, 44003 (2015).
16. B. Paroli, E. Chiadroni, M. Ferrario, and M. A. C. Potenza, "Analogical optical modeling of the asymmetric lateral coherence of betatron radiation," *Opt. Exp.* **23**, 29912 (2015).
17. B. Paroli, E. Bravin, S. Mazzoni, G. Trad, and M. A. C. Potenza, "A modified two-slit interferometer for characterizing the asymmetric lateral coherence of undulator radiation," *Europhys. Lett.* **115**, 14004 (2016).
18. B. Paroli, E. Chiadroni, M. Ferrario, and M. A. C. Potenza, "A systematic study of the asymmetric lateral coherence of radiation emitted by ultra-relativistic particles in laser-driven accelerators," *Nucl. Instr. Meth. Phys. Res. A* **839**, 1–5 (2016).

1. Introduction

Interferometry is widely used in different fields of research [1]. It allows to achieve very high angular resolution in astronomy [2,3] and provides unique quantitative metrology capabilities in biology and medicine [4]. Interferometers are also used to measure the transverse properties of relativistic particle beams using synchrotron radiation (SR) [5] from visible light [6] to soft and hard X-rays [7–9]. Since the SR from a small beam has better spatial coherence, this method is suitable for measuring a small beam size in a non-destructive manner [10]. These methods have been developed since many years. Recently, very robust, unprecedented results have been reported using a smart lens-coupled detection scheme in the x-ray regime [11].

In many cases of interest the source is incoherent and characterized by a broad-spectrum radiation. The possibility to recover information about the intensity profile of such incoherent sources is related to the measurement of the spatial coherence exploiting the van Cittert-Zernike theorem [12–14]. For instance, the spatial coherence of a quasi-monochromatic radiation can be measured using a double-slit interferometer by interposing a narrow band filter or monochromator and recording the visibility of fringes in the interference pattern. However, in such band-limited system the intensity is drastically reduced with respect to the intensity provided by the full-spectrum radiation.

We have recently shown that the transverse properties of a source can be deduced with high sensitivity by means of the peculiar properties of asymmetric lateral coherence of broadband radiation [15–17]. The result is obtained by a measurement of the coherence properties of radiation with an asymmetric interferometer based on a modified double-slit interferometer. The quantities that are measured are both the modulus and the real part of the complex degree of coherence, defined as

$$\gamma_c(\tau) = \frac{\Gamma(\vec{X}; \vec{X}_0; \tau)}{[\Gamma(\vec{X}_0; \vec{X}_0; \tau)\Gamma(\vec{X}; \vec{X}; \tau)]^{1/2}} \quad (1)$$

where:

$$\Gamma(\vec{X}; \vec{X}_0; \tau) = \lim_{T \rightarrow \infty} \frac{1}{2T} \int_{-T}^T E(\vec{X}, t + \tau) E^*(\vec{X}_0, t) dt$$

is the correlation function of the electric field E (x component). The point $\vec{X} = (x, y, z_0)$ is referred to a Cartesian frame where z_0 is a position along the propagation axis z . \vec{X}_0 , placed within the detection plane, is the reference position for evaluating the coherence and $\tau = 0$ elsewhere. As demonstrated in our previous papers [17, 18] the ability to resolve transverse non-uniformities in the radiation source and to measure the beam size is related both to the broad-spectrum of radiation and to the spatially asymmetric detection method. Simulations performed for undulator radiation [17] show that the asymmetric lateral coherence can be used to resolve two spatial separated sources from a large distance.

In this paper we report the results of the first experimental study of the asymmetric lateral coherence properties of radiation by using the real part of the coherence factor γ_c . Known, calibrated sources have been realized by illuminating pinholes of different sizes with a broad-spectrum halogen lamp. A complete two-dimensional mapping is realized for each source by means of measuring the two-point correlation function in the transverse plane (along the x axis) through a systematic scan method. We obtain a good quantitative agreement between experimental results and calculations. Moreover a characteristic structure in the map can be observed, namely a bifurcation of the real part of the coherence factor along a given line, when a structured source (double pinhole) is used instead of a single pinhole. We find that the separation between the two arms of the bifurcation is related to the transverse geometry of the source. This effect has similar behavior to those described in our recent studies on the asymmetric lateral coherence of undulator radiation [17], suggesting the possibility to apply the experimental

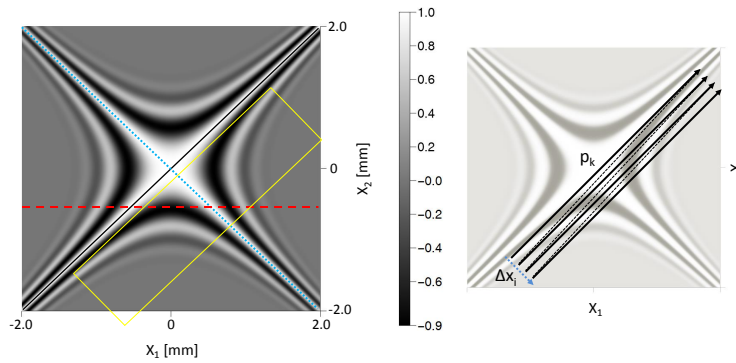


Fig. 1. (Left) Two-dimensional map of $Re\gamma_c(x_1, x_2)$ calculated using a circular source with diameter $50\ \mu\text{m}$. Black solid line where $x_1 = x_2$ is the main diagonal $Re\gamma_c = 1$. The section along the blue dotted line $x_1 = -x_2$ gives the spatial coherence as measured by a classical two-pinhole interferometer. The asymmetric lateral coherence is obtained along straight lines with constant x_2 (e.g the red dashed line). The yellow box delimits the portion of the map accessed by the measurements described in this work. (Right) A diagram of the scan strategy using the coordinates p_k and Δx_i . The solid arrows (black) show the increment of p_k for each slit separation Δx_i , which increases at each scan along the dashed arrow (blue).

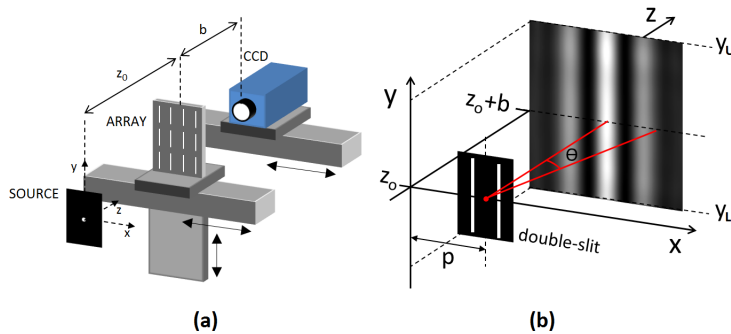


Fig. 2. (a) Schematic representation of the experimental setup. Three linear stages are used to scan the radiation in the transverse plane $x - y$. (b) Geometry of the measuring system (double-slit interference pattern) within the reference frame (x, y, z) .

method to synchrotron-like sources. In general, the method can be used to characterize broadband sources with the following advantages:

- i) The possibility to measure source size with a sensitivity higher than a classical Young's interferometer (which in addition needs radiation with limited bandwidth).
- ii) The ability to accurately resolve the separation between nearby sources, i.e. a direct measurement of the distance between the bifurcation arms (in the real space) instead of the indirect measurement (in the spatial frequency domain) by means of the van Cittert-Zernike theorem.
- iii) The possibility to use the van Cittert-Zernike theorem without the need to limit the radiation spectrum (no need to measure the fringe visibility).

The paper is organized as follows. In section 2 we discuss the properties of the asymmetric lateral coherence map. The experimental setup and data analysis are presented in section 3. Section 4 is devoted to results and discussions. Finally we collect our conclusions in section 5.

2. Two dimensional mapping

Let's assume that a quasi-homogeneous incoherent source is centered at the origin of the frame (x, y, z) where x is the horizontal direction, y is the vertical direction and z is the axis of propagation. We can characterize the transverse coherence in the far field using a double-slit interferometer by increasing the distance between two slits positioned along the x axis and centered on the optical axis z . For a quasi-monochromatic radiation the visibility of the interference pattern as a function of slit separation (for a quasi-monochromatic radiation) gives the modulus of the complex degree of coherence $|\gamma_c|$. The real part of γ_c can be also measured to obtain the phase information by increasing the distance between the slits and recording both visibility and phase ϕ of the interference pattern, so that $Re\gamma_c = |\gamma_c| \cos \phi$. Even though this method provides useful information about transverse coherence properties of the radiation field, it involves only the radiation field at the positions characterized by symmetry $(x_1, x_2 = -x_1)$, where x_1, x_2 are independent variables of the points $\vec{X} = (x_1, 0, z_o)$, $\vec{X}_0 = (x_2, 0, z_o)$ introduced above (see Eq. 1) and z_o is the distance between the source and the detection plane along the optical axis z .

For this work we realize a more complete characterization of the transverse coherence through a 2-dimensional map of the real part of γ_c for all possible combinations of x_1, x_2 in a given interval around z_o . An example of such a map obtained with a circular broadband source with diameter $50 \mu\text{m}$ and $z_o = 57 \text{ cm}$ is shown in Fig. 1 where $Re \gamma_c(x_1, x_2)$ is computed from Eq. 1. Here a gaussian power spectral density with half-power bandwidth $\Delta\nu = 2.1 \cdot 10^{14} \text{ Hz}$ is used in the calculations. In this more general context and consistent with the definition in [17] we define the real part of the asymmetric lateral coherence $A_s(x_1)$ for a fixed reference value $x_2 = x_0$ as $A_s(x_1) = Re \gamma_c(x_1, x_2 = x_0)$, i.e. an horizontal profile of the map (see red dashed line in Fig. 1). On the contrary, the real part of the coherence factor obtained from a classical interferometer, as discussed above, is the profile of the map $S_c(x_1) = Re \gamma_c(x_1, x_2 = -x_1)$ along the diagonal shown by the blue dotted line, where $2|x_1|$ is the separation between the slits. Information provided by the 2D map is much more rich than that obtained with a classical interferometer as demonstrated in the experiments described below. In fact, only structures characterized by symmetry $(x_1, x_2 = -x_1)$ are observable by a classical Young's interferometer.

3. Experimental setup and method of analysis

In principle, the two-dimensional mapping of the asymmetric lateral coherence can be simply obtained by using two slits vertically oriented along the y axis so that the relative position can be changed independently along the x direction. With the first slit fixed at x_2 , the other one is placed at different positions x_1 along the x axis, thus increasing the slits separation. Each scan of x_1 should be repeated for each value of x_2 to provide a complete 2-dimensional mapping accordingly with Eq. 1. In order to achieve the necessary accuracy in positioning both slits we fabricated an array of double-slits with different spacing Δx_i ($i = 1 \dots 36$). The map is obtained through the transformation $(x_1, x_2) \rightarrow (p_k + \frac{\Delta x_i}{2}, p_k - \frac{\Delta x_i}{2})$, where p_k ($k = 1 \dots 69$) is the position of the double-slit center along the x axis. A complete mapping can be also realized by changing the position p_k for each spacing Δx_i of the array as shown in Fig. 1 (right).

In Fig. 2 (a) we show a sketch of the experimental set-up. The source is a circular aperture illuminated by a halogen lamp (Mod. USHIO EKE 21V150W). The slit separation Δx_i changes between $200 \mu\text{m}$ and 1.6 mm in steps of $40 \mu\text{m}$ with each slit $50 \mu\text{m}$ wide. Measurements were performed with three sources: two single pinholes (with diameter $50 \mu\text{m}$ and $200 \mu\text{m}$) and two identical pinholes with diameter $200 \mu\text{m}$ spaced by $240 \pm 10 \mu\text{m}$. The distance of the slits from the source was $z_o = 57 \text{ cm}$. Two linear stages positioned the array in the transverse plane $x - y$. The interference pattern produced by the double-slits was detected with a cooled, low-noise, Charge Coupled Device (CCD, Mod. PCO1600) at a distance $b = 500 \text{ mm}$ from the

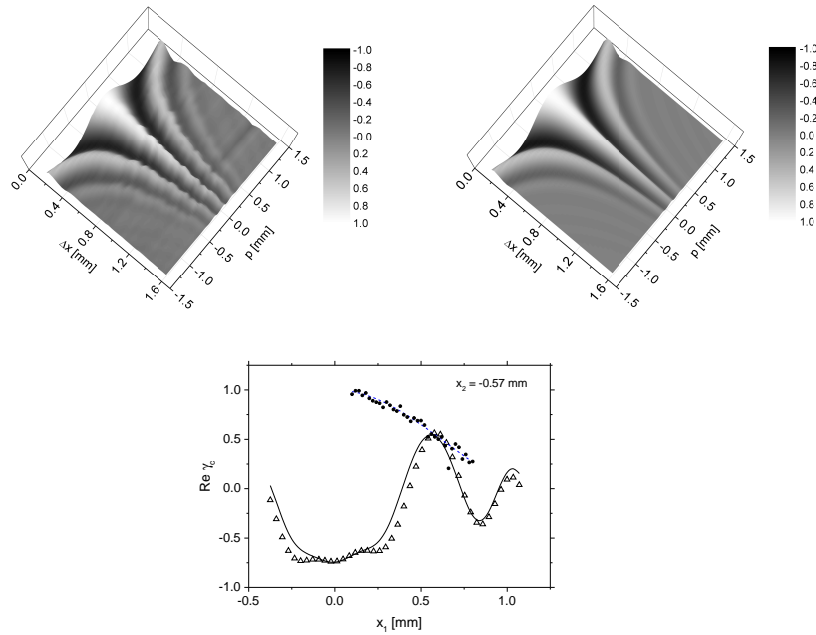


Fig. 3. Experimental results (top left) for $Re \gamma_c(x_1, x_2)$ with a $200 \mu\text{m}$ pinhole compared to the calculated map (top right). Bottom: experimental profiles for the asymmetric lateral coherence $A_S(x_1, x_2 = -0.57\text{mm})$ (triangles), and for the classical Young's interferometer $S_C(x_1)$ (circles) compared to the corresponding theoretical results (black solid line and blue dashed line, respectively).

slits. Interference patterns were analyzed numerically to extract $Re \gamma_c$ as described below.

The 2-dimensional patterns $P'(x, y)$ recorded by the CCD were integrated along the y direction to increase the signal to noise ratio. The integrated patterns can be described by the function,

$$P(\theta) = \int_{y_L}^{y_U} P'(p + \theta b, y) dy,$$

where $\theta \approx (x - p)/b$ is the observation angle and y_L, y_U are the lower and upper limits of the CCD frame, respectively (see Fig. 2 (b)). The real part of the complex degree of coherence can be written as [12]:

$$Re \gamma_c(\tau) = \frac{P(\theta) - I_1(\theta) - I_2(\theta)}{2\sqrt{I_1(\theta)I_2(\theta)}} \quad (2)$$

where $I_1(\theta)$ and $I_2(\theta)$ are defined as:

$$I_1(\theta) = \int_{y_L}^{y_U} I_1'(p + \theta b, y) dy,$$

$$I_2(\theta) = \int_{y_L}^{y_U} I_2'(p + \theta b, y) dy$$

and $I_1'(x, y), I_2'(x, y)$ are the diffraction patterns of each individual slit at the detector. With the approximation $I_1(\theta) \approx I_2(\theta)$ and defining $S(\theta) = I_1(\theta) + I_2(\theta)$, we write

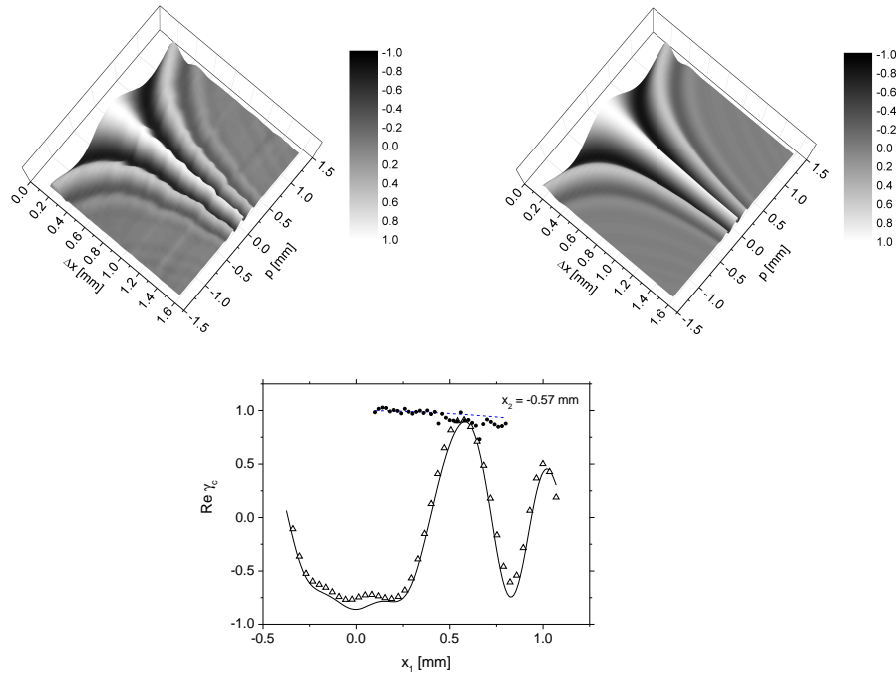


Fig. 4. Experimental results (top left) for $Re \gamma_c(x_1, x_2)$ with a $50 \mu\text{m}$ pinhole compared to the calculated map (top right). Bottom: experimental profiles $A_s(x_1, x_2 = -0.57\text{mm})$ (triangles), $S_c(x_1)$ (circles) compared to the corresponding theoretical results (black solid line and blue dashed line, respectively).

$$Re \gamma_c(\tau) = \frac{P(\theta)}{S(\theta)} - 1. \quad (3)$$

Equation 3 demonstrates that two quantities must be measured to evaluate $Re \gamma_c$, i.e. the integrated pattern $P(\theta)$ and $S(\theta)$ which is measured illuminating each double-slit through a light diffuser to guarantee the condition of spatially incoherent illumination. In this way we still measure the integrated pattern $P(\theta)$, but now $Re \gamma_c = 0$ due to the incoherent illumination so that Eq. 3 gives $S(\theta) = P(\theta)$. Finally the values of $Re \gamma_c(\tau = 0)$ were obtained from Eq. 3 posing $\theta = 0$ (zero path length difference) after subtracting the background from each pattern.

4. Results and discussion

In this section we first show the experimental results obtained for the case of single circular sources. We then discuss the results obtained with two pinholes, showing that the present method is capable to resolve separated sources in a way different from classical methods.

Maps are obtained as discussed in section 3 for the $Re \gamma_c$ region evidenced in Fig. 1. The maps are symmetric with respect to the main diagonal (black solid line of Fig. 1):

$$Re \gamma_c(x_1, x_2) = Re \gamma_c(x_2, x_1). \quad (4)$$

In Fig. 3 we show experimental results (left) for the map of the asymmetric lateral coherence of a $200 \mu\text{m}$ pinhole compared with the calculated map (right) obtained from Eq. 1. The raw

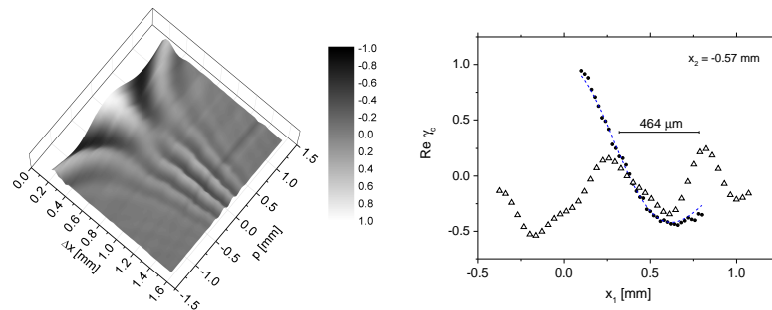


Fig. 5. Experimental results (left) of $Re \gamma_c(x_1, x_2)$ using a double pinhole ($200 \mu\text{m}$ diameter, $240 \mu\text{m}$ spacing). A bifurcation is clearly present along $p = 0$ for $\Delta x_i \approx 0.7 \text{ mm}$. Right: experimental profile $A_s(x_1, x_2 = -0.57 \text{ mm})$ (triangles). Notice that around $x_1 = 0.57 \text{ mm}$ (corresponding to the reference point $x_2 = -0.57 \text{ mm}$) due to bifurcation two maxima appear instead of one as in Fig. 3. The distance of $464 \mu\text{m}$ between maxima is in good agreement with the expected value obtained from the pinhole separation. The experimental profile $S_c(x_1)$ (circles) compared with theory (blue dashed line) is also shown.

data show small fluctuations mainly due to the imbalance between the slit pairs. The maximum imbalance occurs for a slit separation $\Delta x_i = 1.32 \text{ mm}$ which gives a discrepancy of about 20% with respect to theory. In Fig. 3 (bottom) we show the two main profiles $A_s(x_1)$ (asymmetric lateral coherence, triangles) and $S_c(x_1)$ (classical interferometer, circles) which are in good agreement with the theoretical curves (black solid line and blue dashed line, respectively). Notice that the limited scan region (see yellow box in Fig. 1) does not exhibit the symmetry of the profiles A_s and S_c .

Results obtained with the $50 \mu\text{m}$ pinhole are shown in Fig. 4. Due to the small size of the aperture the light intensity at the detector was very low, almost comparable with the background noise. Nevertheless this is not a true limitation for the measurements. The spatial coherence along the profile $S_c(x_1)$ (circles) is in good agreement with theory (blue dashed line) until $x_1 \approx 0.46 \text{ mm}$. Data are then affected by a small systematic depression. This can be attributed to changes of the background during measurements due to the translation of the position stages. Background effects can be demonstrated to add a constant term c to $P(\theta)$, resulting in an offset term added to the coherence factor $Re \gamma_c + \frac{c}{S(0)}$.

Results obtained with two pinholes are also in good agreement with the calculated profiles $A_s(x_1)$ of the asymmetric lateral coherence. The shape of A_s depends on the source size: for example the amplitude at $x_1 = 0.57 \text{ mm}$ (symmetric with respect to the reference point $x_2 = -0.57 \text{ mm}$) decreases as the diameter of the pinhole increases. Similar results was observed in our recent paper [17] where a 2-dimensional Monte Carlo simulation with an ensemble of 10^4 particles was performed in order to measure the transverse size and anisotropies of proton beams propagating through the superconducting undulator of the LHC synchrotron light monitor at CERN. The undulator was modelled as a weak plane undulator with harmonic field of period length $\lambda_u = 28 \text{ cm}$, field strength $B_0 = 5 \text{ T}$ and periods $N_u = 2$. Random gaussian distributions of emitters with transverse size between $100 \mu\text{m}$ and $400 \mu\text{m}$ was generated. Radiation was computed using the Lienard-Wiechert formula. The real part of the asymmetric lateral coherence of the free-propagating radiation was characterized at 12 m and 28 m from the radiation source.

Our observation confirms results obtained from simulations. We find that the amplitude of the maximum (symmetric with respect to the reference point) has a similar dependence (with respect to the source size) despite the different emission processes.

Moreover a two particles model was described in simulation in order to deduce the effect of

separation between two nearby sources. In such model we consider the two particles separated by a distance $2x_d$, where $\pm x_d$ are the transverse positions with respect to the undulator axis, respectively. The analysis of the wavefront of radiation emitted by particles separately (on the detector plane) show that two adjacent maxima distant $4x_d$ should be observed in the real part of the coherence factor; i.e. at a distance two times greater than the distance between particles. We show the same effect by using two separated pinholes.

The shape of the profile A_s also provides further information about structured sources as shown in Fig. 5, where a double pinhole both diameters of $200 \mu\text{m}$ was used as the source. A symmetric bifurcation is clearly observable on the map at $\Delta x_i = 0.7 \text{ mm}$, $p = 0 \text{ mm}$. The bifurcation is related to the transition between the near field (Fresnel region) and the far field (Fraunhofer region). It can be roughly shown comparing the separation between the adjacent maxima with their characteristic spatial period $2d \approx \sqrt{\lambda z_o}$ which provides $z_o \approx 4d^2/\lambda$. In such condition the location of the bifurcation point can be observed when the slit separation is comparable or greater than the spatial period, $\Delta x_i \geq \sqrt{2\lambda z_o}$, where the factor $\sqrt{2}$ is the projection of Δx_i along the profile of the asymmetric lateral coherence. The bifurcation is the origin of the additional maxima also observed in [17]. They are generated when the profile $A_s(x_1)$ is extracted from the map. The $464 \mu\text{m}$ distance between the adjacent maxima (see Fig. 5 (right)) is a factor 2 larger than the pinhole separation $d = 232 \mu\text{m}$. This magnification was predicted by the two particles model [17] applied to undulator radiation. We obtain the same magnification assuming the pinhole separation as analogous to the distance between particles. We stress that no bifurcation is observable along the profile $S_c(x_1)$, although the pinhole distance can be estimated using the Van Cittert-Zernike theorem as shown in Fig. 5 (right). Here the experimental data (circles) fitted with the theoretical curve (blue dashed line) are in good agreement with a pinhole distance of $232 \mu\text{m}$.

5. Conclusions

We have shown in this work a novel approach that exploits an array of double slits to characterize thermal sources providing a complete 2D map of the two-point correlation for the radiation field. The real part of the complex degree of coherence is directly measured in order to preserve the phase information. The proposed method does not rely on the classical monochromatic measurement of fringe visibility. Instead, the asymmetric lateral coherence A_s is measured using higher intensity wide-spectrum radiation.

We experimentally demonstrate that the amplitude and shape of the asymmetric lateral coherence function depend on the source size, which can be accurately measured by fitting the calculated map to the data. We obtain good agreement between expectations and experiments, the discrepancy with respect to expected values is mainly given by the background noise and by the uncertainty of the positioning stages.

Moreover the proposed method is capable of providing information about structured sources. In fact the $232 \mu\text{m}$ distance between two pinholes was measured by simply taking the distance between the two arms of the bifurcation produced by the source non-uniformity. Such distance is a magnification of a factor two.

The strong analogy with similar results obtained in our previous work using synchrotron-like radiation [17] suggests that the proposed method can be extended and applied to other sources of radiation.

Funding

Italian Ministry for University and Research (MIUR) "FIRB 2012" funds (RBFR12NK5K).